The International Journal of Advanced Manufacturing Technology (2018) 99:1993–2003
https://doi.org/10.1007/s00170-018-2541-5

ORIGINAL ARTICLE

Formability of titanium alloy sheets by friction stir incremental forming

P. A. Grün[1] · E. H. Uheida[2] · L. Lachmann[1] · D. Dimitrov[2] · G. A. Oosthuizen[2]

Received: 3 April 2018 / Accepted: 8 August 2018 / Published online: 30 August 2018

Abstract
This paper investigates the behavior of titanium formability when forming under localized friction heating, caused by high tool rotation. In accordance with planned experiments, different process conditions at various tool rotations, feed rates, and step-down sizes were investigated. The experiments were carried out on 1 mm thick Ti6Al4V alloy sheets, using an 11 mm diameter, ball-ended tooltip. The rotational speeds were designed to create sufficient thermal effect, while maintaining high lubricity at the forming interface. Moderate tool rotational speed (2000 rpm) tends to improve formability, reduce the forces, and lower the rate of tool wear. The experimental procedures are presented, and an extensive discussion of the results is reported.

Keywords Frictional heating · SPIF · Ti6Al4V · Tool wear

1 Introduction

As a result of a combination of attributes like corrosion resistance, high strength-to-weight ratio, and biocompatibility, titanium alloys are employed in diverse engineering applications. Using thin-wall designs together with the mechanical properties of this alloy results in applications with a lower structural weight and an enhanced performance [1, 2]. Titanium alloys on the other hand, even in the annealed condition, are problematic to form at room temperature. Low-speed, superplastic forming at elevated temperatures (750–950 °C) is typically used for the fabrication of Ti6Al4V sheets. The process allows the production of complex and precise geometries, but implies special-purpose and expensive tools [3].

Single point incremental forming (SPIF) is a de facto dieless technology for forming sheet metal. In SPIF, a sheet is essentially formed by the application of a small punch driven by a standard CNC milling machine. Significant flexibility and reductions in tolling cost can be realized from such novel technology, which is dedicated to the reduction of the buy-to-fly ratio, and to broadening the range of small series product applications of titanium. There are, however, several process issues that still need to be improved before a wider SPIF industrialization can take place [4]; these are issues such as slow processing speed, poor geometric precision, high residual stresses, and constrained forming limits.

In recent literature, the capability of SPIF in fabricating hard-to-form alloys has been investigated, by testing differing hybrid variations of the process. These variations involved heat-assisted SPIF. In some of these hybrid variations, heat energy was applied by conducting a high DC current via the forming tool onto the sheet; this procedure is referred to as electrically assisted incremental sheet forming [3, 5–7]. In other cases, the workpiece was locally heated by a dynamic laser beam spot [8–12]. More recently, Ambrogio et al. [13] investigated an innovative hot SPIF version, where induction heating and cryogenic cooling are dynamically used to enhance the formability of Ti6Al4V samples. In their research work, Xu et al. [14] provide a brief description and

✉ E. H. Uheida
uheida@sun.ac.za; emadoheda@gmail.com

P. A. Grün
Peter.Gruen81@gmx.de

L. Lachmann
lutz.lachmann@htw-dresden.de

D. Dimitrov
dimitrov@sun.ac.za

G. A. Oosthuizen
tiaan@sun.ac.za

[1] Department of Production Engineering, University of Applied Sciences, Dresden, Germany

[2] Department of Industrial Engineering, Stellenbosch University, Stellenbosch, South Africa

classification of the hybrid methods for both local and global heating of workpieces produced by SPIF. These hybrid techniques exhibited significant improvements in material formability, but there is a substantial increase in both the equipment cost and the process complexity.

However, mindful of the objectives of maintaining process flexibility and cost efficiency, a direct heating method called friction stir incremental forming [15, 16] was utilized in this study. This method entails embossing the sheet by means of a tool spinning at relatively high speeds, causing frictional heating of the sheet. Curiously, the applications of this approach are mainly found in technical literature that focuses on aluminum and steel sheets. There is a dearth of information on hard-to-form materials such as titanium alloys, which are suited to customized, high-value components, produced in small batches. Ambrogio et al. [17] investigated the effect of the tool feed rate and the step depth on temperature variations at the forming interface, during the SPIF of titanium Ti6Al4V sheets and aluminum alloy (AA5754) sheets. For the same forming conditions, additional heat generation is associated with the forming of titanium samples. The study was conducted using a lath machine and free rotating tool, thus deviating slightly from a standard SPIF process done typically on a milling machine [18].

This paper experimentally investigates friction stir incremental forming of Ti6Al4V, while considering reasonable settings for the process variables. The investigating methodology included the design of a test benchmark, with the test platform having been established, based on encouraging formability results from a previous study on SPIF of grade 2 titanium sheets [18]. In the sections following, a brief description of the materials and procedures is presented, followed by a discussion of the observations.

2 Material and method

Figure 1a depicts the custom-developed, blank-holding fixture, attached to a force dynamometer, and mounted on a CNC table. The fixture design makes it possible to do four runs consecutively for a single test setup; when compared to four individual tests, this effects a saving on material and a reduced setting-up time per test. All test samples were waterjet cut from annealed 1-mm-thick Ti6Al4V alloy sheets. The sample sheets were square with side length 190 mm, and they were attached symmetrically over the four working areas of the blank-holding fixture. A clamping torque of 50 Nm was applied to the M12 bolts of the clamping plate.

For the test benchmark, a conical frustum with a varying wall angle was selected. The benchmark CAD model shown in Fig. 1c had a depth of 25 mm and a maximum internal diameter of 56 mm. By design, the wall angle (θi: degrees) of the sample profiles increases proportionately to the sample depth (h_i : mm) as measured along the vertical z-axis—this is given by Eq. 1. This was made to minimize the effect on material formability that might result from the rate at which the wall angle changes as the forming depth increases [19].

$$\theta_i = 30^{\circ} + 1.8 \cdot h_i \tag{1}$$

The research samples were formed by applying uniform step-down increments, together with a 3D tool path, spiraling from the outer diameter to the middle. From the CAD/CAM packages marketed by Delcam, PowerSHAPE and PowerMILL 2016 were respectively used to generate the benchmark CAD geometry and the forming tool path. A climb milling strategy, where the tool moves counterclockwise while it rotates around its axis in a clockwise direction, was implemented. An additional four runs were made using a conventional milling strategy, where the tool feed and rotation were in the same direction. An 11-mm spherical tooltip made of C45k steel (a medium carbon steel) is hardened to 57 HRC and polished. A hemispherical, 10-mm-diameter forming tooltip, made from tool steel 2312 and heat-treated using a TUFFTRIDE process, was used in the one-factor-at-a-time test. A titanium aluminum nitride (TiAlN) nanocoating, which is a surface treatment that offers added protection against heat, friction, and abrasion,

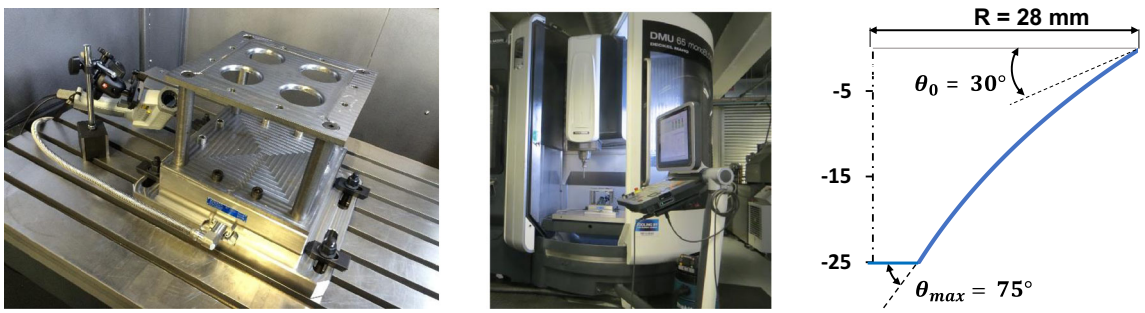

Fig. 1 Depiction of the SPIF test setup: the blank-holding fixture **a** attached to Kistler 9255C and **b** mounted on a CNC table. **c** the benchmark profile

was applied to protect the working surface of the tooltips. For lubrication, 98.5% molybdenum disulfide powder was applied. The solid lubricant was ideal to meet the specific requirements of the material (Ti6Al4V), the test set-up, and the measuring devices used.

Data of the forming temperature and force were continuously recorded for the full duration of the processing time. The forming forces were obtained using a stationary table-type Kistler 9255C dynamometer (Fig. 1a) mounted below the forming fixture. The dynamometer was paired to a Kistler 5070A 8-channel signal amplifier. The components of forming forces were recorded using a type 5697 DAQ data card and DynoWare software.

A field radiation-based method was used to measure the surface temperature, by means of a Ranger MX4 infrared pyrometer. The pyrometer has a temperature range −30°C to 900°C and ± 1°C accuracy. Such a method obviates undesirable impacts on the forming process. It enables tracking of the temperature as the motion of the tool moves the contact area, vertically downwards, on the side of the component being formed. To intensify the pyrometer readings of the forming temperature, the undersides of the sheets were sprayed with heat-resistant paint to improve and unify the emissivity of the titanium. The pyrometer was calibrated to match the emissivity of the sprayed specimens. The calibration was done using thermocouple and DataTemp MX software. As shown in Fig. 1a, the pyrometer was mounted onto a movable tripod that has a magnetic base, so it could be moved easily to maintain its optimal measuring distance every time it was repositioned for a certain test run.

Throughout a test run, the temperature was not recorded for the entire component geometry, but only on one side of the component. Considering that the test components formed are axisymmetric, and that the heat is generated only by friction and deformation, it is assumed that there was an equivalent rise in temperature all along the contour path of each forming pass [20].

Testing by means of the one-factor-at-a-time (OFAT) and the design-of-experiment (DoE) methods were used to establish the strength of the correlations between the kinematics of the tool and the formability of the Ti6Al4V sheets. The DoE test involved 14 runs, with a single replicate on the three process parameters: step depth (Δz), the feed rate (f), and the rotation speed (n). The forming tooltip is understood to be a key design factor that interacts with the other parameters and can significantly affect the forming outputs. In selecting a tool (material and size), factors such as blank thickness, material strength, and the size of minimum feature to be formed must be considered. As per collected data from literature and in-house experience, tooltip diameters predominately applied were between 8 and 12 mm [21]. In this range, it was found that the preferred diameter to the blank thickness ratio is about 10. Hence, 11- and 10-mm tooltips were respectively used in the DoE and the OFAT tests. Main values for the test parameters were then selected related to the tooltip size, the model material, and profile—these values are Δz 0.5 mm, f 1050 mm/min, and n 2000 rpm. Throughout the DoE, each value was ranged by a fixed interval around the anticipated optimal setting. The OFAT experiments involved 16 runs, with four levels of the three process parameters tested. The Δz test was repeated using a conventional milling strategy (n and f had the same direction). The settings of each test are described accordingly in Sect. 3.

Process factors like the sheet thickness, the material type, geometry, the friction conditions, and the type of tool path were presumed constant. The Design-Expert 10 software was used to generate the layout of the experiments, as well as for the post-process analysis. Experiments were performed according to the planned layout. If an obvious sheet fracture or

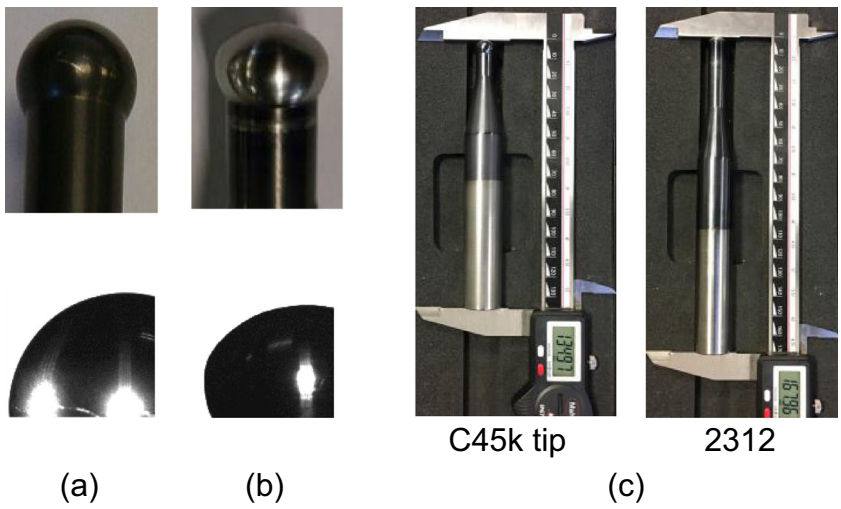

Fig. 2 The forming tools with TiAlN-Nano coating showing **a** C45k tooltip before test, **b** removal of coating and wear after test, and **c** decreased length of the C45k tool by 1.06 mm and the 2312 tool by 1.44 mm

Table 1 Types of the tooltip maintenance procedure

Type	Tooltip condition	Tool maintenance procedure
1	Minor tool wear	Tool is mounted to the CNC and rotated at 2000 rpm, while tooltip is manually cleaned using a fleece.
2	Moderate tool wear and friction welding	Tool is mounted to the CNC and rotated at 1000 rpm, manually cleaning in three steps: - using a grinding stone - using P200, P600, and P1200 grit sandpaper - polishing with P1200 grit sandpaper + oil, at 2000 rpm
3	Severe tool wear and friction welding	Tool is demounted from the CNC and manually cleaned: - using a grinding machine - following the procedures given for type 2

tooltip overheating was observed during the experiment, the test run was terminated; if not, the test was stopped upon reaching the design depth of 25 mm. After every test run, measurements of the forming depth (h) achieved were taken. Maximum formability as judged by the forming angle (θ°) was then found using the model given by Eq. 1.

3 Results and discussion

During the experiments, major processing challenges came from overheating of the forming interface. Another issue was the sticking of titanium to the tooltip, blemishing the smoothness of the contact profile. In the worst-case scenario, friction welding of titanium sheeting to the tooltip occurred. Figure 2 illustrates the forming tools used and highlights the wear conditions observed.

Because of the elevated temperatures caused by increased friction at the forming interface, both the removal of the material and the oxidation of the formed surface were escalated. It was necessary to inspect the tooltip after every test run to confirm the operating condition of the tool. In most cases, the tooltip surface had to be cleaned and polished to counter the resulting wear. Table 1 shows the maintenance procedures followed, related to the type of tooltip wear experienced.

3.1 Results from the DoE test

Table 2 summarizes the investigated parameters and the maximum response data resulted in each test run. Forming results were considerably correlated to the level of the rotational speed used. The discussions of the test results are set according to the three levels of the rational speed (low, medium, and high) tested.

Table 2 The DoE layout and summary of the results

Test run		Parameter			Response maximum value			
Sample no.	ID no.	f (mm/min)	n (rpm)	Δz (mm)	T (°C)	F (N)	h (mm)	θ (°)
1	1	600	500	0.35	52	272	4	37.1
2	0	1050	2000	0.50	480	1247	25	75.0
3	0	1050	2000	0.50	306	952	22.3	70.1
4	8	1500	3500	0.65	492	1048	4	37.3
5	0	1050	2000	0.50	578	1201	25	75.0
6	2	1500	500	0.35	57	1053	4.2	37.5
7	7	600	3500	0.65	246	464	0	30.0
8	0	1050	2000	0.50	587	785	21.1	68.0
9	3	600	3500	0.35	272	626	2.8	35.0
10	4	1500	3500	0.35	330	1264	2.5	34.6
11	6	1500	500	0.65	37	252	2.4	34.3
12	5	600	500	0.65	54	910	3.5	36.3
13	0	1050	2000	0.50	477	1574	9.6	47.3
14	0	1500	2000	0.50	524	1118	20.2	66.3

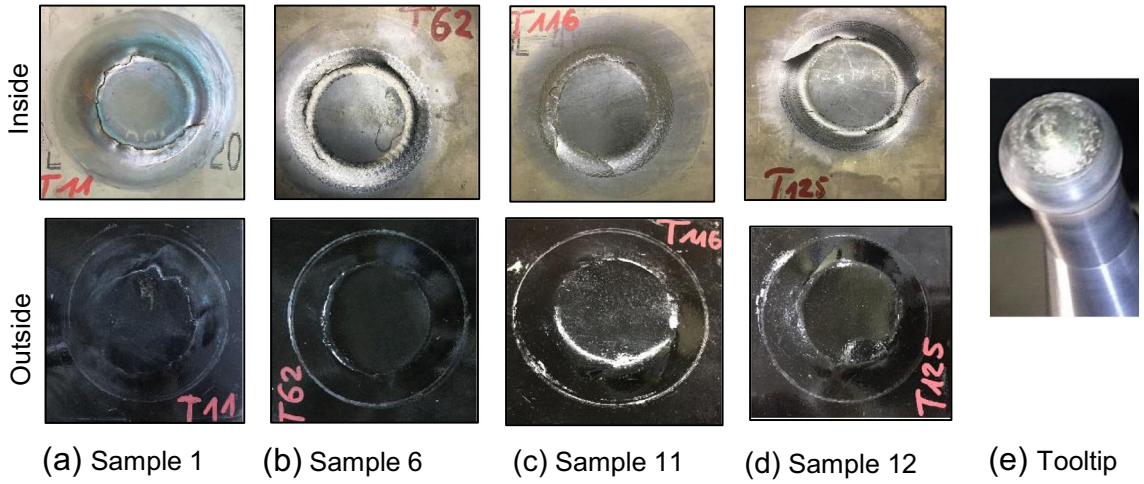

Fig. 3 Results obtained at n 500 rpm and different f and Δz: **a**–**d**, samples cracked with low material formability; **e** tool wear condition type 1

Four of the tests that were conducted at low rotation (n:500 rpm) and different feed and step depth levels had to be aborted before the full cycle time, due to the failure of the sample. Figure 3 illustrates the inside and outside of samples 1, 6, 11, and 12, which cracked shortly after the start of the test, with almost no significant deformation. The tooltip exhibited minor wear as shown in Fig. 3e; after each run, it had to be polished in accordance with the type 1 maintenance procedure.

The maximum forming angle obtained at the low rotation remained low ($\theta < 40^{\circ}$). Temperature gradients for these samples are shown in Fig. 4a. Throughout these tests, maximum temperatures did not exceed 60 °C.

Unlike the preceding results discussed, samples 2, 3, 5, 8, 13, and 14 which were shaped at a medium rotational speed of 2000 rpm displayed a higher formability. After undergoing, virtually, the full 25-mm design depth, samples 3, 8, and 14 failed. Failure in form of sheet cracks that occurred close to the sample bottom was mainly due to sheet over-thinning. Samples 2 and 5 were formed without failure, while run 13 was accidently terminated. This level of formability is unique in so-called single-pass incremental forming, where using an 11-mm tooltip on 1.0-mm Ti6Al4V sheets, a wall angle of 75° can be achieved. Example of the formed samples and the wear condition experienced on the tooltip are illustrated in Fig. 5.

Temperature gradients measured for these samples are shown in Fig. 4b. The fluctuations (spikes) seen on the temperature curves are due to the heat source (interface) changing its relative position to the measuring spot of the pyrometer. The instant readings were a maximum, when the tooltip was processing the material directly above the measuring spot. These readings were a minimum, when the tooltip was forming the far side of the component, diametrically opposite to the measuring spot. The frequencies at which these spikes occurred increased with deepening component depth, because of the reduction in the component diameter. As the diameter

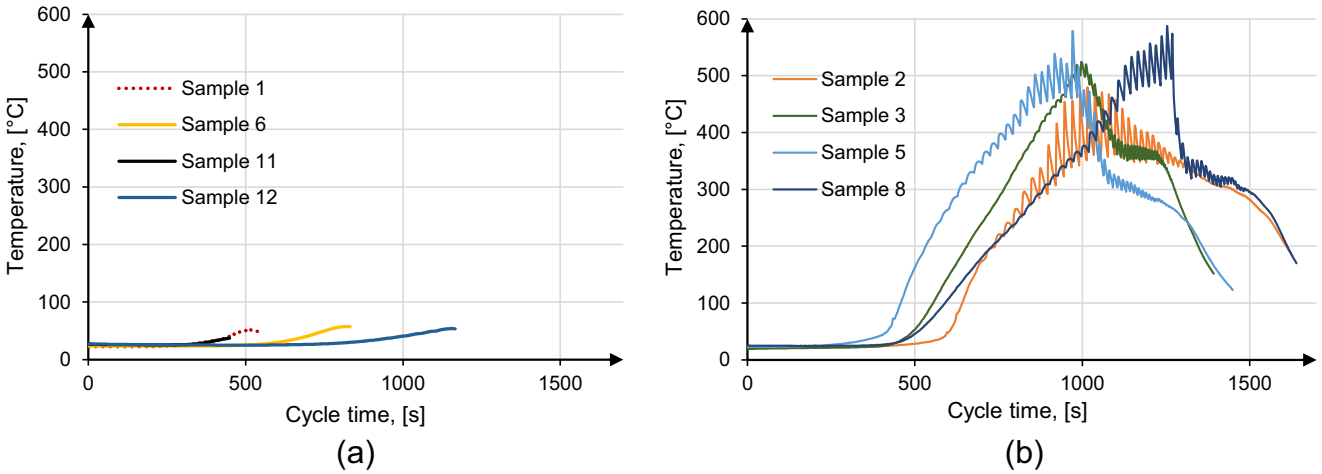

Fig. 4 Temperature gradients obtained at different forming conditions: (a) at low rotation n : 500 rpm and various f and Δz; **b** n : 2 000 rpm; f : 1050 mm/min ; Δz : 0.5 mm

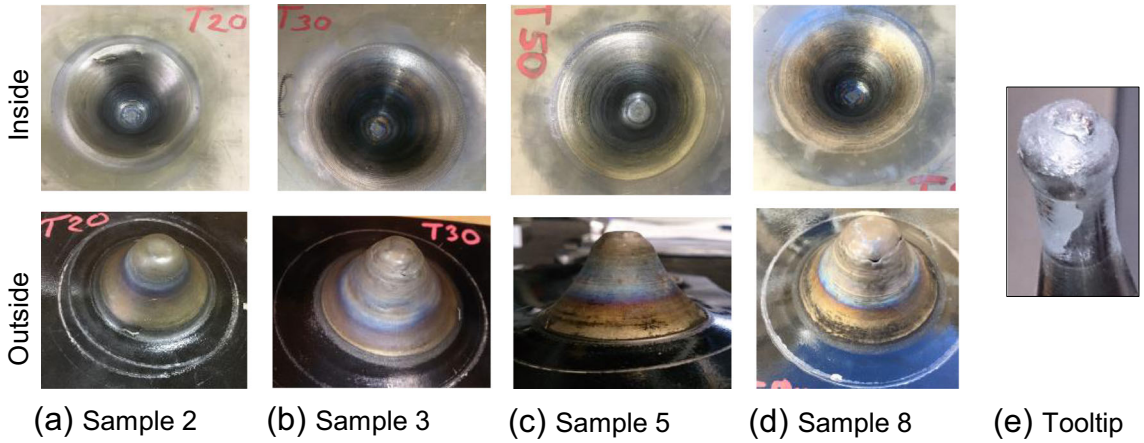

Fig. 5 Results obtained at medium speed (n : 2 000 rpm): **a**–**d**, samples formed close to the design shape; **e** tool wear condition type 2

becomes smaller, at a constant feed rate the heat source sweeps past the measuring spot more rapidly.

As shown in the Fig. 4b, the deformation was associated with a localized rise in temperature, which averaged values at the developed range of deformation, extended from 400 to 460 °C. The heat was mostly accumulated along the swept surface, due to the poor rate of heat dissipation as a result of the low conductivity of the Ti6Al4V sheets. The localized build-up of heat facilitated the shaping process, because the resulting thermal softening enhanced the ductility of the samples.

Qualitative assessment of the samples internally revealed rough surfaces, resulting from material removed by wear. On the outside of the samples, oxidation of the titanium material because of overheating was evident. The effect was intensified near the bottom of the samples (material color change in Fig. 5) which is consistent with the ascending gradients of the forming temperature measured. On two counts, the latter effect can be linked to the profile that was formed: as the forming depth increases, the sample wall angle increases, and the diameter of the sample decreases. The first factor enlarged the tool/sheet contact area, while the second increased the tooltip sweeping frequency of the interface, as the tool path shortened. At a constant feed rate and small step depth, these factors augmented the frictional heat generated. Consequently, the generated heat is concentrated near the bottom of the samples, because of the stated higher sweeping rate and the decrease in dissipation time.

Figure 5e shows an example of the tooltip condition after forming at the moderate rotation speed of 2000 rpm. The wear and titanium buildup on the contact surface of tooltip were a manifestation of the high forming temperature and pressure. Upon completion of each test run, the maintenance procedures for type 2 wear was implemented to restore the working condition of the tooltip.

Samples 4, 7, 9, and 10 were produced at the relatively high rotation of 3500 rpm and various levels of feed and step depth. As shown in Fig. 6, the samples failed dramatically, with almost no significant plastic deformation of the titanium. Instead, a

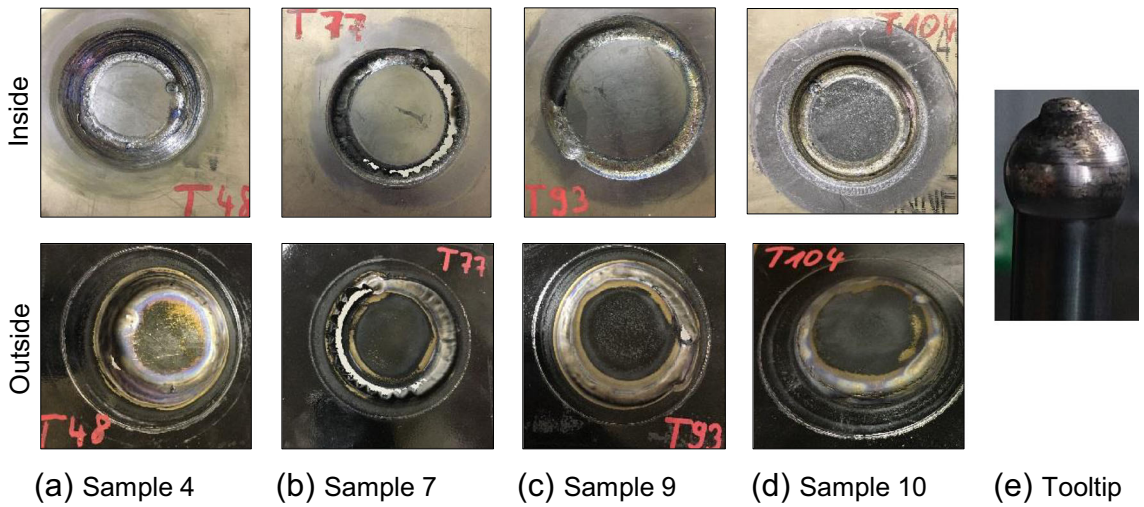

Fig. 6 Results obtained at high 3500 rpm and different feed and step levels: **a**–**d** samples failed by excessive removal of material; **e** an example of type 3 tooltip wear

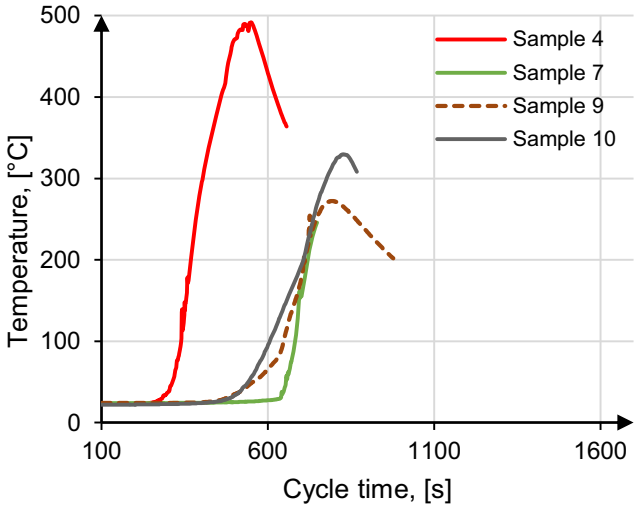

Fig. 7 Steep temperature gradients resulted at n : 3 500 rpm and various f and Δz levels

milling-like effect took place on their respective forming interfaces. Each of the forming tests had to be terminated after a short period, because of the excessive removal of the material, or the penetration of the tooltip into the sample material.

For these samples, temperature at the interface rapidly escalated to the range of 400–500 °C (sample 4 with the highest f and Δz settings) and triggered glowing of the tooltip and ignition of the shaved titanium particles. Despite the early termination of these forming tests, significant frictional welding of the titanium was occurred on the tooltip (Fig. 6e). After each test run, the tooltip had to be demounted from the CNC spindle, ground, and polished in accordance with the exhaustive, type 3 maintenance schedule. As shown in Fig. 7, comparable steep gradients were resulted for samples 7, 9, and 10, but at different points on the cycle time subjected to $f$and Δz used (refer to Table 2).

The DoE results displayed a significant effect of n on the forming outputs. Samples shaped at the lower or higher n exhibited early failure with minimum formability regardless of the level of f or Δz used. Contrarily, at the medium level of n samples, formability improved, mainly by the reduced sliding friction force, and the amount of heat generated at the contact locus. From the preceding discussion and referring to the test data in Table 2, there is only a particular combination (ID 0) of the parameter settings that facilitated the decent formability—the settings are n = 2000 rpm, f = 1050 mm/min, and Δz = 0.5 mm.

3.2 Main effect of parameters

To further investigate the effects of the process variables on Ti6Al4V formability, each of the forming parameters, f, n, and Δz was individually investigated over a wider range, while the other two parameters were kept constant at their respective reference levels. This eliminated the possible impact of interaction between parameters on the outcomes. Throughout the OFAT test, the values f = 625 mm/min, n = 1940 rpm, and Δz = 0.3 mm were set as the reference values for the parameters. The range and reference level were chosen from a previous in-house study on SPIF of grade 2 titanium sheets [22, 23]. This was made to allow evaluating and understanding the two material behavior and effect on outputs, via comparing results between the two studies under similar forming conditions.

3.2.1 The effect of the rotational speed

Four rotation speeds, namely, 450, 900, 1500, and 2500 rpm were tested. The produced samples are shown in Fig. 8. A comparable result set to that of the above-discussed DoE tests

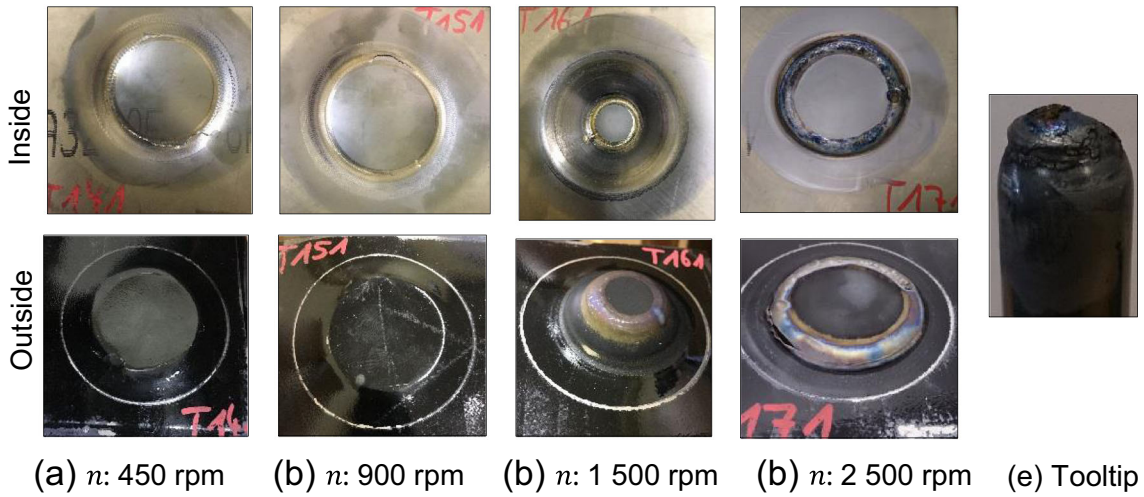

Fig. 8 Results from OFAT: **a**–**d** the effect of n on the formability while keeping f and Δz at their reference values; **e** type 3 tooltip wear resulted at 2500 rpm

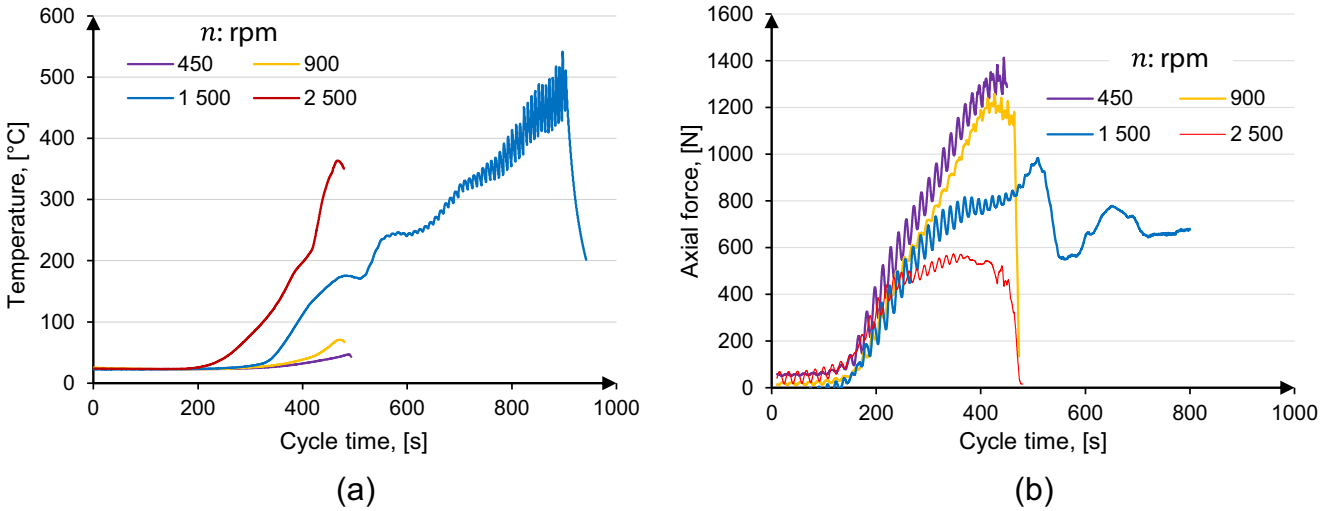

Fig. 9. Results from the OFAT test showing the relationship between rotational speed and **a** temperature and **b** axial force

were found concerning material formability and wear. Only at the 1500 rpm was an increased deformation achieved. At the both rotation extremes, rapid sheet failure by fracture, or by severe wear of the interface, occurred.

At the low rotations of 450 and 900 rpm, the maximum temperatures were respectively 47 and 71 °C. At such low temperatures, insufficient heat generated in the forming zone resulted in reduced formability of the samples. By contrast, overheating of the material at the interface occurred when n was 2500 rpm. Severe friction welding developed on the tooltip (Fig. 8e), which escalated material removal from the workpiece surface and resulted in rapid failure. At $n = 1500$ rpm, an adequate heating effect facilitated enhanced formability with less deterioration of the material at the contact interface. Figure 9 illustrates the gradients of temperature and axial force measured in the rotation tests, showing reduced axial force at higher n relative to the evolved test temperature.

3.2.2 Effect of the feed rate

In these tests, the feed rate f was stepped from 1200 up to 10,000 mm/min, while keeping the other variables at their reference values. The four samples shown in Fig. 10a–d failed with reduced formability. Quality deterioration of sample surface intensified, as the feed rate increased. A slight wear of the tooltip (type 1) was observed at each of the four levels of the feed speed.

The graphs in Fig. 11 plot a comparison of the temperature, and axial forces gradients observed at the f values tested.

Concerning maximum temperature measured during the feed test, the highest temperature was 212 °C at the lowest feed rate of 1200 mm/min. The maximum temperature significantly dropped to 60 °C at the largest f, which was accompanied by a slight increase in the axial force by about 200 N. The reduced temperature can be related to the shedding opportunity of localized heat, which is transferred to and builds up in the

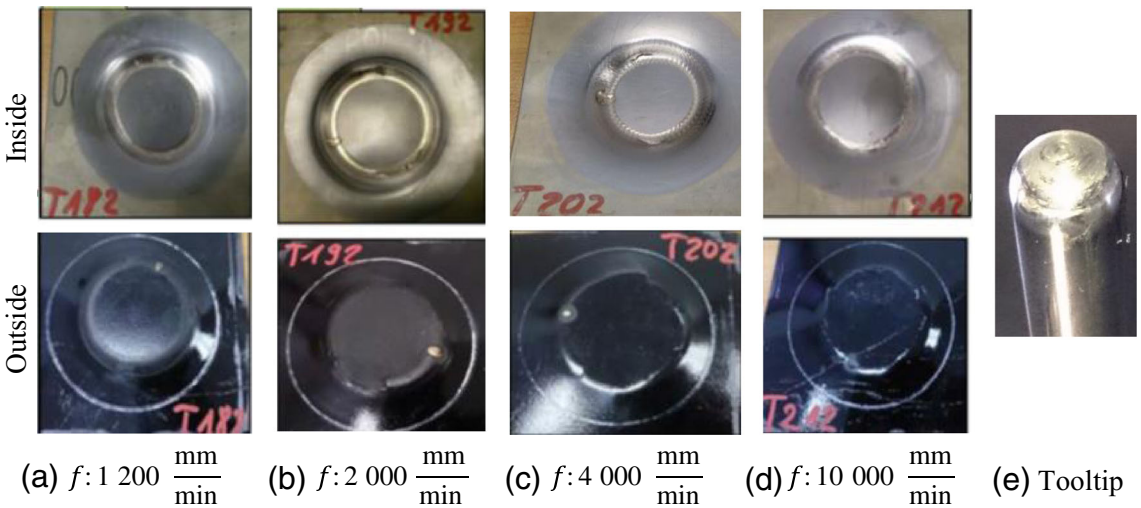

Fig. 10 Results from the OFAT test showing **a**–**d** the effect of f on the formability keeping n : 1 940 rpm and Δz 0.5 mm; **e** type 1 tooltip wear

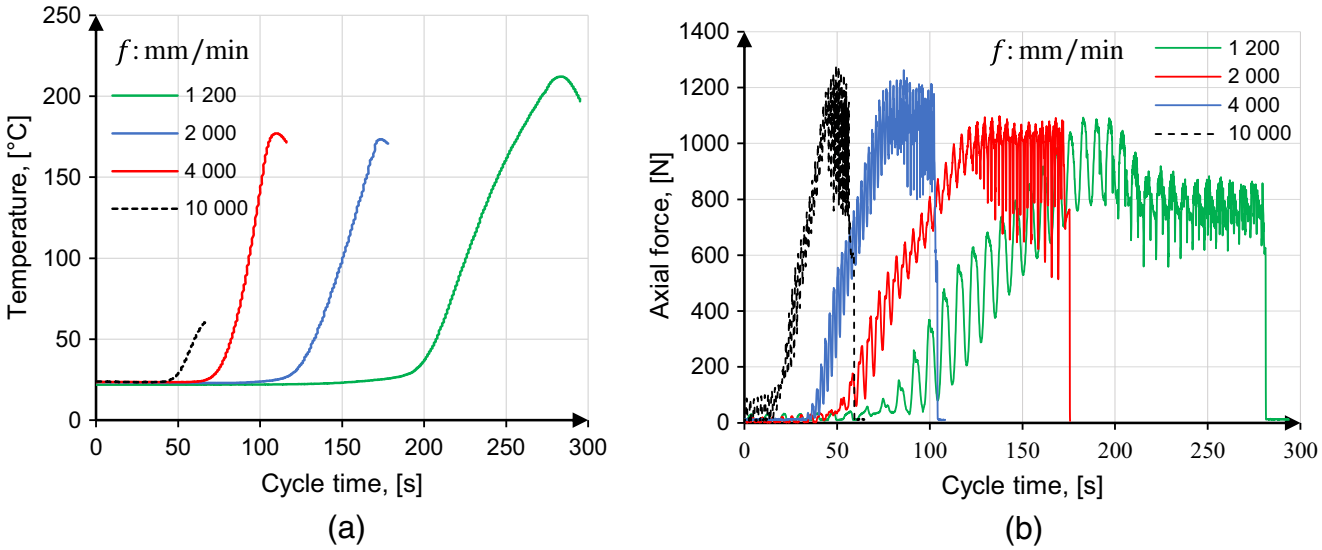

Fig. 11 Results from the OFAT test showing the relationship between the feed rate and **a** forming temperature and **b** axial force

material at high tool feed rates. The heat source provided by the rotating tooltip rolls faster over the contact surface and more heat is dissipated, than is accumulated on a specific area. The low formability and rise in force at large *f* can therefore be attributed to the reduced heating, which remained small at the forming interface.

On experimental testing at elevated speeds, the CNC machine (a gantry type with max speed of 40,000 mm/min) could not uphold the programmed (10,000 mm/min) feed; the machine exhibited oscillating feeds caused by acceleration and deceleration and kinematic characteristics. In high-speed machining of complex with short segment trajectories to precisely follow the profile, the machine slows down and sometimes oscillates imitating natural vibration. During the tests, that might also violate the heating process by altering the contact mechanisms at the interface, resulting in temperature drop and increased forces. Consequently, arguments cited in literature [17, 24, 25] on using high feed rates to mitigate the SPIF challenges of speed and productivity may not always be relevant or applicable.

3.2.3 Effects due to the step depth size and rotation direction

Four step depth levels were tested, namely, Δ*z* 0.35, 0.5, 0.65, and 0.8 mm, both in climbing and conventional strategies; the results are depicted in Fig. 12.

Low formability limits were obtained, with the maximum forming depth of the eight runs confined to a narrow band. As the step size increased, there was a slight reduction in the maximum temperature, together with a rising trend of the axial force. Since the samples failed at narrow forming depths, the decrease in temperature may be related to reduced cycle time (heating) when step size was increased. Figure 13a presents a comparison of the temperatures and axial forces, as resulted from the climbing and conventional strategy. For legibility

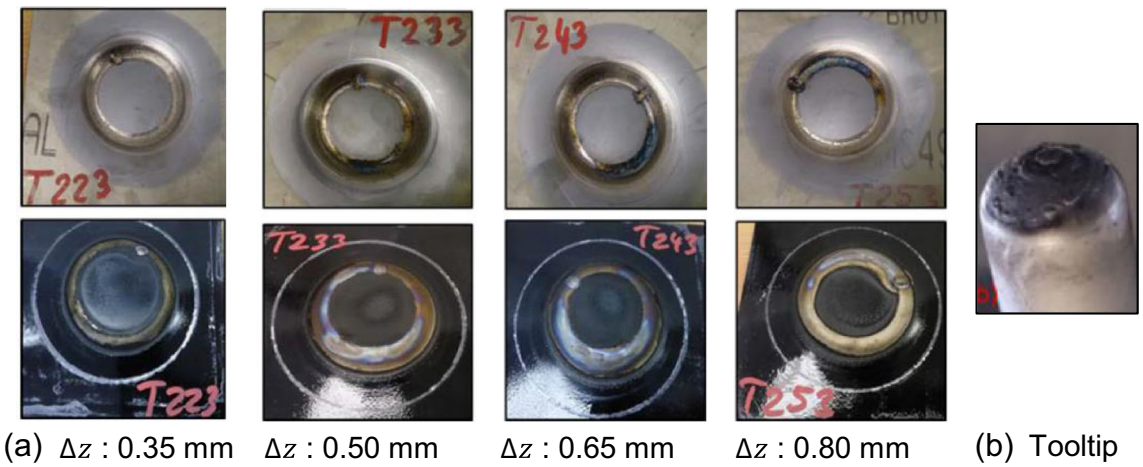

Fig. 12 Results from OFAT test showing **a** effect of Δ*z* on formability and **e** type 2 wear on the tooltip

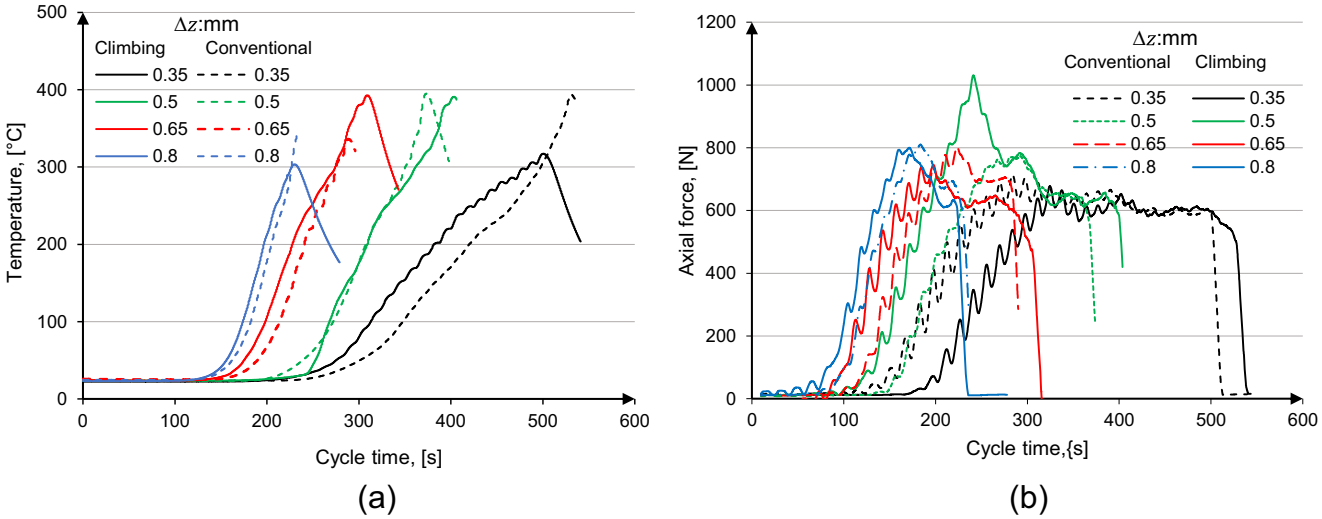

Fig. 13 Relationship between Δz and forming output as resulted from the climbing and conventional strategies. **a** forming temperatures. **b** axial forces

and contrast of results, the moving average filter was used to smooth out the data in the graphs.

When compared to the marginal effects noted for the conventional strategy, the results from the climbing strategy over the same stepping range were very similar in terms of variation in temperature and forces. This is in contrast to findings related to the grade 2 titanium sheets reported in [22], to which considerable effects on formability, geometric accuracy, forming forces, and forming temperature between the two forming strategies (climb and conventional) were observed.

The preceding analysis of results from the OFAT showed that independently varying the input parameters over a wider range did not facilitate good formability results. This suggests that interactions of SPIF parameters play a significant role on the output, more so than one-factor effects.

4 Conclusions

This paper investigated friction stir incremental forming of Ti6Al4V alloy sheets. The influences on the forming output of three key process parameters, namely, the rotation speed n, the feed rate f, and the step depth Δz, were studied; both the DoE and OFAT types of experiments were used. Considering the investigated range of the variables and the benchmark geometry formed on 1-mm-thick Ti6Al4V alloy sheets, using an 11-mm-diameter, ball-ended tooltip, the following conclusions can be drawn:

- Tool rotation speed is the dominant process parameter, determining the thermal effect and the associated material formability and forming force. The level of the feed rate and step depth both revealed a minor impact.
- Improved formability and reduced wear at the interface can be achieved in the working range of $n = 2000$ rpm, $f = 1050$ mm/min, and $\Delta z = 0.5$ mm.
- Low formability limits and rapid failure of the titanium samples are mostly anticipated outside this working range. Failure results either by brittle-cracking of the titanium at a low temperture when using a low n or due to severe friction welding and the removal of material from the interface using a relatively high n.

Besides the unique and encouraging level of the Ti6Al4V formability achieved in this study, there are also serious quality problems with the process that need to be addressed. The use of shielding gas (similar to metal welding processes) for protecting the freshly formed surfaces against oxidation and the testing of ultra hard tooltips are both research-worthy topics that have not been explored, and that can enhance the SPIF of highly reactive and hard-to-form titanium alloys.

Acknowledgments The Stellenbosch Technology Centre staff members are acknowledged for their contribution to the experimental work.

Funding information This study was financially supported by the South African Department of Science and Technology.

References

1. Novakova L, Homola P, Kafka V, Materials A (2014) Effect of structure on properties of incrementally formed titanium alloy sheets. Int J Mech Aerospace Ind Mechatronics Eng 8(2):371–376
2. Palumbo G, Brandizzi M (2012) Experimental investigations on the single point incremental forming of a titanium alloy component combining static heating with high tool rotation speed. Mater Des 40:43–51
3. Fan G, Gao L (2014) Mechanical property of Ti-6Al-4V sheet in one-sided electric hot incremental forming. Int J Adv Manuf Technol 72(5–8):989–994
4. Allwood JMM, Duncan SRR, Cao J, Groche P, Hirt G, Kinsey B, Kuboki T, Liewald M, Sterzing A, Tekkaya AEE (2016) Closed-loop control of product properties in metal forming. CIRP Ann Manuf Technol 65(2):573–596
5. Fan G, Gao L, Hussain G, Wu Z (2008) Electric hot incremental forming: a novel technique. Int J Mach Tools Manuf 48(15):1688–1692
6. Fan G, Sun F, Meng X, Gao L, Tong G (2009) Electric hot incremental forming of Ti-6Al-4V titanium sheet. Int J Adv Manuf Technol 49(9–12):941–947
7. Liu R, Lu B, Xu D, Chen J, Chen F, Ou H, Long H (2016) Development of novel tools for electricity-assisted incremental sheet forming of titanium alloy. Int J Adv Manuf Technol 85(5–8):1137–1144
8. A Mohammadi, H Vanhove, A Van Bael, JR Duflou (2013) Influence of laser assisted single point incremental forming on the accuracy of shallow sloped parts. In: NUMISHEET 2014, 864–867
9. Callebaut B (2008) Sheet metal forming by laser forming and laser assisted incremental forming. KU Leuven, Leuven
10. SAA Member, ET Akinlabi (2013) Experimental investigation of laser beam forming of titanium and statistical analysis of the effects of parameters on curvature. II
11. Mosecker L, Göttmann A, Saeed-Akbari A, Bleck W, Bambach M, Hirt G (2013) Deformation mechanisms of Ti6Al4V sheet material during the incremental sheet forming with laser heating. Key Eng Mater 549:372–380
12. Duflou JR, Callebaut B, Verbert J, De Baerdemaeker H (2007) Laser assisted incremental forming: formability and accuracy improvement. CIRP Ann Manuf Technol 56(1):273–276
13. Ambrogio G, Gagliardi F, Chamanfar A, Misiolek WZ, Filice L (2017) Induction heating and cryogenic cooling in single point incremental forming of Ti-6Al-4V: process setup and evolution of microstructure and mechanical properties. Int J Adv Manuf Technol 91(1–4):803–812
14. Xu DK, Lu B, Cao TT, Zhang H, Chen J, Long H, Cao J (2016) Enhancement of process capabilities in electrically-assisted double sided incremental forming. Mater Des 92:268–280
15. Buffa G, Campanella D, Fratini L (2013) On the improvement of material formability in SPIF operation through tool stirring action. Int J Adv Manuf Technol 66(9–12):1343–1351
16. Otsu M, Katayama Y, Muranaka T, Otsu TMM, Katayama Y (2014) Effect of difference of tool rotation direction on forming limit in friction stir incremental forming. Key Eng Mater 622(623):390–397
17. Ambrogio G, Gagliardi F (2015) Temperature variation during high speed incremental forming on different lightweight alloys. Int J Adv Manuf Technol 76(9–12):1819–1825
18. Uheida E, Oosthuizen G, Dimitrov D (2017) Investigating the impact of tool velocity on the process conditions in incremental forming of titanium sheets. Proc Manuf 7(2016):345–350
19. Khalatbari H, Iqbal A, Shi X, Gao L, Hussain G, Hashemipour M (2015) High-speed incremental forming process: a trade-off between formability and time efficiency. Mater Manuf Process 30(11):1354–1363
20. Xu D, Wu W, Malhotra R, Chen J, Lu B, Cao J (2013) Mechanism investigation for the influence of tool rotation and laser surface texturing (LST) on formability in single point incremental forming. Int J Mach Tools Manuf 73:37–46
21. E Uheida, G Oosthuizen, D Dimitrov (2016) Toward understanding the process limits of incremental sheet forming of titanium alloys. In Proceedings, COMA16' Int. Conf. on Competitive Manufacturing, 27–29 January 2016 Stellenbosch, South Africa pp. 161–172
22. Uheida EH, Oosthuizen GA, Dimitrov DM, Bezuidenhout MB, Hugo PA (2018) Effects of the relative tool rotation direction on formability during the incremental forming of titanium sheets. Int J Adv Manuf Technol 96:3311–3319
23. Ambrogio G, Gagliardi F, Bruschi S, Filice L (2013) On the high-speed single point incremental forming of titanium alloys. CIRP Ann Manuf Technol 62(1):243–246
24. Hamilton K, Jeswiet J (2010) Single point incremental forming at high feed rates and rotational speeds: surface and structural consequences. CIRP Ann Manuf Technol 59(1):311–314
25. Ambrogio G, Filice L, Gagliardi F (2012) Improving industrial suitability of incremental sheet forming process. Int J Adv Manuf Technol 58:941–947